CrossMark

ORIGINAL PAPER

Microwave properties of natural rubber based composites comprising conductive carbon black/silica hybrid fillers

Ahmed A. Al-Ghamdi[1] · Omar A. Al-Hartomy[1] · Falleh R. Al-Solamy[2] ·
Nikolay Dishovsky[3] · Mihail Mihaylov[3] · Nikolay Atanasov[4,5] ·
Gabriela Atanasova[4,5] · Diana Nihtianova[6]

Abstract Hybrid fillers have been prepared by impregnation of conductive carbon black with different amounts of silicasol, equivalent to 3 % and 7 % silica, respectively. The fillers have been characterized and their effect upon the microwave properties of natural rubber based composites has been also investigated. The results obtained show that, the silica (dielectric) phase is distributed both over the surface and inside the carbon black aggregates (conductive phase). Thus, the interaction between the particles of the conductive filler (building of conductive pathways) is restricted. It has been established that the microwave properties studied are dependent on the ratio between the filler's phases. The composites filled with the hybrid filler comprising the highest amount of silica possess the best total shielding effectiveness and absorptive shielding effectiveness. In all cases absorption is the mechanism prevailing in effectiveness. Thus, the fillers obtained allow an easy control and tailoring of the elastomer based electromagnetic interference shielding materials. The investigations carried out reveal the good potential of the composites studied for finding applications as antennas, automobiles, sensors and military-related applications.

✉ Nikolay Dishovsky
dishov@uctm.edu

[1] Department of Physics, Faculty of Science, King Abdulaziz University, Jeddah 21589, Saudi Arabia

[2] Department of Mathematics, Faculty of Science, King Abdulaziz University, Jeddah 21589, Saudi Arabia

[3] Department of Polymer Engineering, University of Chemical Technology and Metallurgy, 1756 Sofia, Bulgaria

[4] Department of Telecommunications, Faculty of Telecommunications and Management, University of Telecommunications and Post, 1700 Sofia, Bulgaria

[5] Department of Communication and Computer Engineering, Faculty of Engineering, South-West University "Neofit Rilski" of Blagoevgrad, 2400 Blagoevgrad, Bulgaria

[6] Institute of Mineralogy and Crystallography, Bulgarian Academy of Sciences, 1113 Sofia, Bulgaria

Introduction

A significant part of the modern electronic devices used in everyday life such as computers, modems, printers, mobile phones, etc., create electromagnetic interference (EMI) that hinders to a great extent the operating of other similar apparatuses in their vicinity [1, 2]. Therefore EMI shielding materials (EMI SM) protecting bio-systems and digital devices from the unwanted effects of electromagnetic waves have been attracting more and more attention of the scientific circles [3–6]. Usually the major mechanism of EMI shielding is reflection. To be an effective reflecting shield, the latter should possess mobile charge carriers (free electrons) interacting with the unwanted electromagnetic waves. Therefore, the tendency of those shields is their being conductive to some extent, although there is no need of their possessing high conductivity. The availability of free electrons in metals makes them the most used EMI shielding materials reflecting effectively the electromagnetic waves. Though, their high density, proneness to corrosion, the lack of enough elasticity and hard processing, limit their application for light weight EMI SM of a sophisticated form [7, 8]. Those drawbacks could be overcome when using different elastomer based composites. However, most of neat elastomers are dielectrics and entirely transparent for electromagnetic radiation, i.e. their EMI shielding effectiveness (EMI SE) is practically zero. That is why, a good
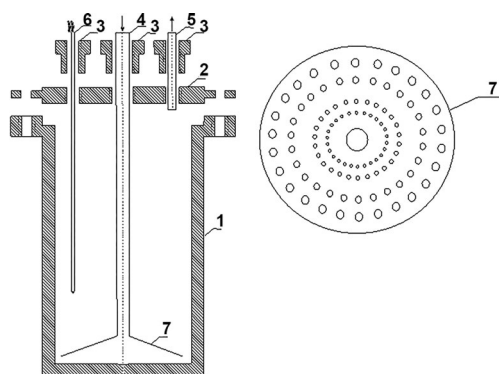
Fig. 1 Design of the reactor used: 1 – Reactor vessel, 2 – Top (Sealing flange), 3 – Sealing nuts, 4 – Gas inlet, 5 – Gas outlet, 6 – Thermocouple, 7 – Buchner funnel

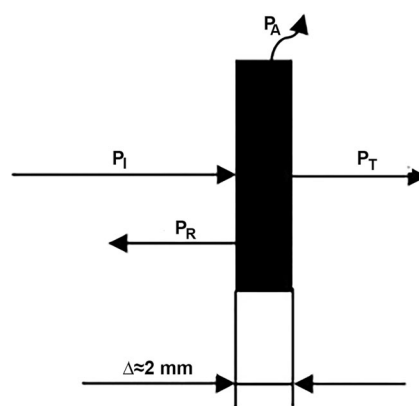**Fig. 2** Schematic presentation of a shielding material interacting with an electromagnetic wave of incident power *(P$_I$)*

elastomer based EMI SM could be obtained only via creation of conductive pathways by introduction of conductive fillers apt to form chain-like structures in the dielectric rubber matrix. Most often such fillers are various metal powders, graphene, conductive carbon black, etc. The high specific surface area of conductive carbon black and its ability to form various aggregates and agglomerates are a key factor in the manufacture of good elastomer based EMI SM [8, 9]. It is also assumed that such elastomer composites should comprise more than 20 phr of conductive carbon black [10].

Another class of elastomer based materials of interest for protecting electronic instruments and equipment are the Rubber Radar Absorbing Materials (RRAMs). RRAMs used as an electromagnetic shielding material that can reduce or weaken EMI in a way. It is mainly made of a rubber matrix and electromagnetic wave absorbents. The absorbents provide the necessary electromagnetic performances of RAM. Rubber is the carrier of the electromagnetic wave absorbents, and it can make a RAM soft, flexible and easy to clip. Thus, many researchers have paid much attention to RRAMs [11, 12]. As known, the main principles for developing elastomer based microwave absorbers are: finding a suitable dielectric rubber matrix and a filler or a system of fillers possessing high dielectric and/or magnetic loss values (such as conductive carbon black,

γ-Fe$_2$O$_3$, Ni-Zn-Fe$_2$O$_4$, Fe$_3$O$_4$, SrFe$_{12}$O$_{19}$, etc.) [13–17]. The crucial factor to obtain good microwave absorbers is the ability of the dielectric matrix or of any other phase to isolate completely the particles of the conducting filler, i.e. its particles to get in fewer contacts with each other [18]. In most cases that requires using the filler in small amounts what has a negative effect upon the mechanical properties of the rubber composites.

It is a fact that a good number of authors have been investigating the microwave properties of composites comprising silica and carbon materials in various forms [19, 20]. That is because the average real part (ε') and imaginary part (ε'') of the relative complex permittivity of silica powder are 4.1 and 0.02 in X-band, i.e. silica is totally transparent for electromagnetic waves what makes it a dielectric matrix appropriate for manufacturing of microwave absorbers [21].

Currently dual-phase furnace carbon black/silica fillers find wider application in rubber industry, particularly in tire manufacturing [22]. The conductivity and dielectric losses of carbon black in the hybrid fillers used in tire production are rather low, hence they could not be used for obtaining elastomer based EMI SM. Solely for that reason it is worth experimenting the impregnation of highly conductive carbon black with silicasol in order to obtain hybrid fillers of different silica amount. It also worth studying the fillers effect upon the microwave properties of natural rubber based composites what has been the main goal of the present work.

According to our working hypothesis, if the silica phase (dielectric phase) in the hybrid fillers is located over the
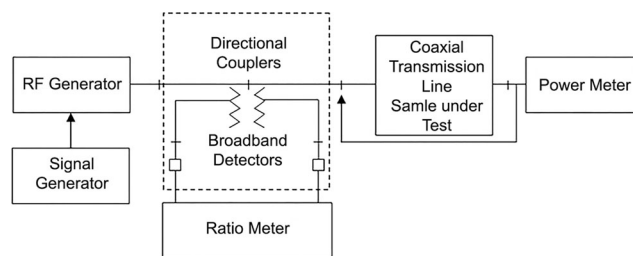
Table 1   Compositions of the investigated natural rubber based composites (phr)

	NR 1	NR 2	NR 3
Natural Rubber – SVR 10	100.0	100.0	100.0
Zinc Oxide	3.0	3.0	3.0
Stearic Acid	2.0	2.0	2.0
Printex XE-2B	70.0	-	-
Pr/Si 3	-	70.0	-
Pr/Si 7	-	-	70.0
TBBS	1.5	1.5	1.5
Sulfur	2.0	2.0	2.0

Fig. 3 Schematic diagram of the system for measuring EMI SE

Table 2   Main properties of the studied fillers

Sample	OAN[a], ml/100 g	IA[b], mg/g	S_{BET}[c], m²/g	S_{MI}[d], m²/g	S_{EXT}[e], m²/g	V_t[f], cm³/g	V_{MI}[g], cm³/g	D_{AV}[h], nm
Printex XE-2B	420	1125	1000	-	-	-	-	-
Pr/Si 3	460	695	912	82	830	1.73	0.04	7.6
Pr/Si 7	480	750	899	76	823	1.70	0.03	7.6

[a] oil absorption number

[b] iodine adsorption

[c] specific surface area (BET)

[d] specific surface area related to the micropores

[e] external specific surface area

[f] the total pore volume

[g] volume of the micropores

[h] the average pore diameter

surface or penetrates the inner domains of conductive carbon black aggregates (conductive phase), it should isolate them and restrict their interaction. Impregnation facilitates an easy control over the quantitative ratio between the dielectric and conductive phases in the hybrid fillers. On the other hand, that ensures an easy control and tailoring the electromagnetic properties of the elastomer composites.

Experimental

Materials

Natural rubber SVR 10 supplied by Hong Thanh Rubber Pty. Ltd. was used as a polymer matrix. The other ingredients such as zinc oxide (ZnO), stearic acid, N-tert-butyl-2-benzothiazole sulfenamide (TBBS) and sulfur (S) were commercial grades and used without further purification.

Hybrid fillers preparation

The hybrid fillers studied were prepared by modification of conductive Printex XE-2B carbon black (by Orion Engineered Carbons GmbH) with silicasol (40 % of silica, pH – 9 and density of 1.3 g/cm³). A mixture of 100 g of Printex XE-2B carbon black and the needed amount of silicasol, corresponding to 3 % or 7 % of silica, was placed into a ball mill and 1.6 l of distilled water was poured over it. The mixture was impregnated for 2 h. The product was placed into a drying chamber at 150 °C and stayed till its complete drying. After that it was ground again in a ball mill for 2 h. Then it was thermally treated at 440 °C under 10^{-2} mmHg vacuum for 2 h in a reactor designed especially for the purpose. Thus the thermal activation could be run at higher temperature without a negative effect upon the carbon black. The design of the reactor used is presented in Fig. 1. Being removed from the reactor the product was ground again in a ball mill and was ready for further investigations. Two hybrid fillers based on Printex XE-2B conductive black and 3 % or 7 % of silica were prepared according to the above method. The fillers were denoted as Pr/Si 3 and Pr/Si 7, respectively.

Preparation of rubber composites

The rubber compounds studied were prepared on a two-roll laboratory mill (rolls Length/Diameter 320 × 160 mm). Table 1 presents the compositions of the rubber compounds studied.
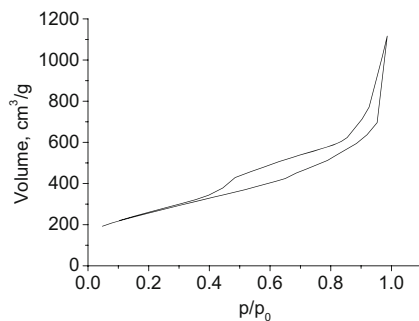

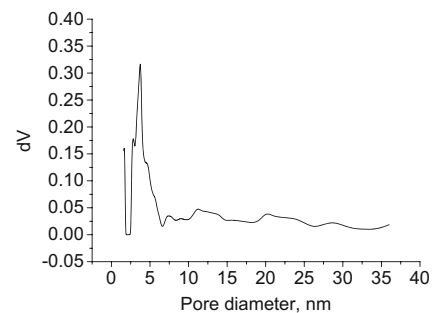**Fig. 4** Volume of adsorbed gas dependence (cm³/g) on relative pressure (p/p₀) of hybrid filler Pr/Si 3

Fig. 5 Derivative volume (dV) as a function of pore diameter (nm) of hybrid filler Pr/Si 3
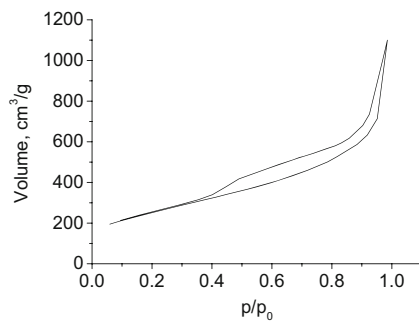
Fig. 6 Volume of adsorbed gas dependence (cm³/g) on relative pressure (p/p₀) of hybrid filler Pr/Si 7

The vulcanization of the natural rubber based compounds was carried out on an electrically heated hydraulic press using a special homemade mold at 150 °C and 10 MPa.

Measurements

Characterization of the studied fillers

The texture characteristics of the studied fillers were determined by low-temperature (77.4 K) nitrogen adsorption in a Quantachrome Instruments NOVA 1200e (USA) apparatus. The nitrogen adsorption–desorption isotherms were analyzed to evaluate the following parameters: the specific surface area (S_{BET}) was determined on the basis of the BET equation, the total pore volume (Vt) was estimated in accordance with the Gurvich rule at a relative pressure close to 0.99. The volume of the micropores (V_{MI}) and the specific surface area related to micropores (S_{MI}), as well as the external specific surface area (S_{EXT}) were evaluated according to V-t-method. Additionally, the pore-size distributions were calculated by DFT method using NLDFT equilibrium model. All samples were outgassed for 16 h in vacuum at 120 °C before the measurements.

For ascertaining the distribution of carbon black and silica, the hybrid products were also investigated by
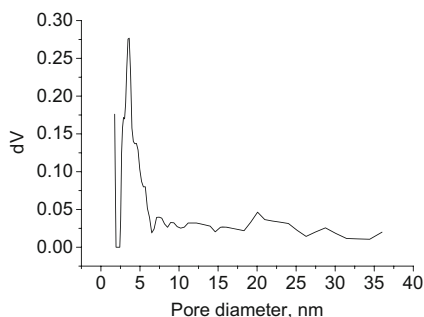

Fig. 7 Derivative volume (dV) as a function of pore diameter (nm) of hybrid filler Pr/Si 7

TEM. The TEM investigations were performed on a TEM JEOL 2100 instrument at accelerating voltage of 200 kV. The specimens were prepared by grinding and dispersing them in ethanol by ultrasonic treatment for 6 min. The suspension was dripped on standard holey carbon/Cu grids. The measurements of lattice-fringe spacing recorded in HRTEM micrographs were made using digital image analysis of reciprocal space parameters. The analysis was carried out by the Digital Micrograph software. TEM JEOL 2100; XEDS: Oxford Instruments, X-MAX^N 80 T; CCD Camera Orius 1000, 11 Mp, Gatan.

Microwave properties measurements

Figure 2 presents the mechanism of interaction of a composite to an electromagnetic wave with incident power P_I. A fraction of the power of the wave reflects back by the surface of the material P_R. Another fraction passes through the material while being absorbed by it and converted into heat P_A, whereas remainder gets transmitted P_T.

The total shielding effectiveness was defined as the ratio between the incident power on the sample P_I and the transmitted power P_T in accordance with Eq. (1) [23–25]:

$$SE_T = 10\log\frac{P_I}{P_T} \tag{1}$$

The total shielding effectiveness (SE_T, in dB) and the reflective shielding effectiveness of the sample surface (SE_R, in dB) were determined by Eqs. (2) and (3) [26–29]:

$$SE_T = -10\lg T, \tag{2}$$

where $T = |P_T/P_I| = |S_{21}|^2$

$$SE_R = -10\lg(1-R), \tag{3}$$

where $R = |P_R/P_I| = |S_{11}|^2$.

S_{11} and S_{21} are complex scattering parameters or S-parameters (S_{11} corresponds to the reflection coefficient and S_{21} - to the transmission coefficient).

The absorptive shielding effectiveness (SE_A) was calculated as the difference between (2) and (3), as shown in Eq. (4):

$$SE_A = SE_T - SE_R \tag{4}$$

The attenuation coefficient (α, dB/cm) was determined using Equation (4). Substituting SE_T and SE_R in it with Eqs. (2) and (3), Eq. (5) is obtained.

$$SE_A = 10\lg\left(\frac{P_I\left(1-|S_{11}|^2\right)}{P_T}\right) \tag{5}$$

Fig. 8 **a** BF- STEM image and compositional maps: **b** Carbon map; **c** Silicon map; **d** Oxygen map of hybrid filler Pr/Si 3
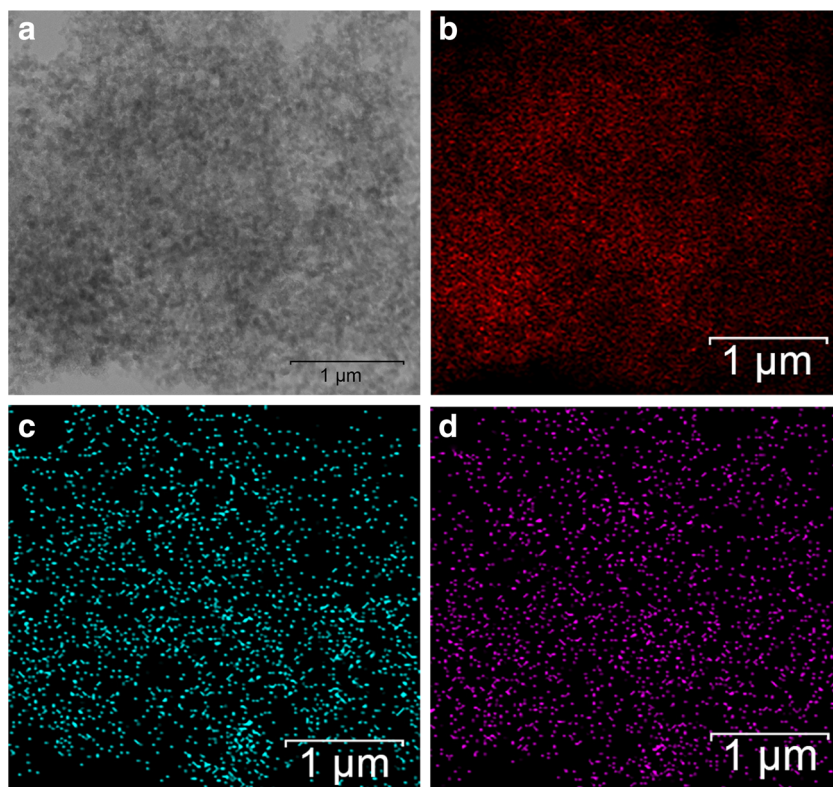

Fig. 9 **a** BF-STEM image and compositional maps: **b** Carbon map; **c** Silicon map; **d** Oxygen map of hybrid filler Pr/Si 7
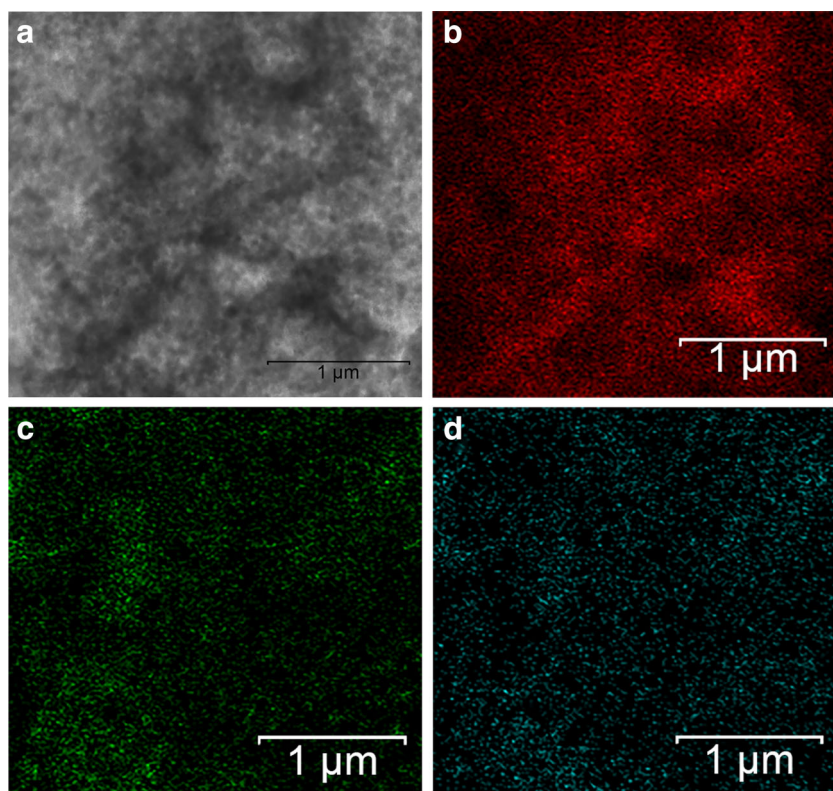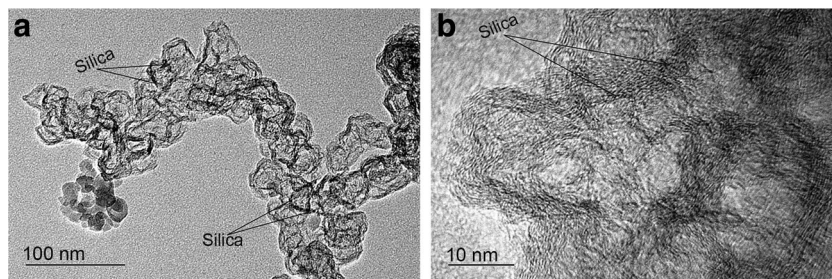
Fig. 10 BF-TEM micrographs of hybrid filler Pr/Si 3 at different magnifications: **a** × 60,000; **b** × 400,000

For determining the attenuation coefficient, Eq. (5) was divided by the thickness of the sample **d** in centimeters, as shown in Eq. (6).

$$\alpha = \frac{SE_A}{d} = 10\lg\left(\frac{P_T}{P_I\left(1-|S_{11}|^2\right)}\right) \tag{6}$$

Figure 3 presents the schematic diagram of the measurement system for the EMI SE in a broadband frequency range. The experimental setup consists of a coaxial reflectometer (coaxial directional couplers Narda model 4222–16 and detectors Narda FSCM 998999 model 4503 A, separating the incident power from the reflected power in the transmission line); a Ratio Meter HP Model 416 A, calculates and depicts the amplitude of the reflection coefficient; a series of radiofrequency generators G4-37 A, G4–79 to G4–82 and HP 68 A in the frequency range from 1 GHz to 12 GHz; a signal generator BM492 releasing a modulating signal at 1 kHz directed towards the radiofrequency generator; a coaxial transmission line Orion type E2M for frequencies from 1 GHz to 5 GHz; a coaxial measuring line APC-7 mm for frequencies from 6 GHz to 12 GHz and a power meter HP 432 A. The cutoff frequencies for the coaxial measuring lines were determined by the formulas presented in literature [30, 31]. The sample holder, reflectometer setup and radiofrequency generator were connected with a rugged phase stable cable N9910X-810 Agilent and through the connectors without interference from other components.

The ratio meter was calibrated prior to carrying out the actual measurements. A calibrating "Open-Short-Load" procedure was applied with Agilent N9330 and Agilent 1250 calibration kits.

Measurements of the incident power, transmitted power and reflection coefficient were performed using the following procedure:

a) Preparation of the measuring system.
b) The system was calibrated with calibration kits in order to eliminate systematic errors from the proper measurement.
c) Preparation of the samples by cutting out pieces from the obtained vulcanized materials having dimensions as follows:

– external diameter of 20 mm and internal diameter of 7 mm in case of using coaxial transmission line Orion E2M;
– external diameter of 7 mm and internal diameter of 3 mm in case of using coaxial measuring line APC-7 mm.

d) Carrying out measurements for determining the module of the reflection coefficient using:

– standard load of the type Agilent 1250, connected in the position of the coaxial line;
– blank coaxial line with a standard load at the end (Agilent N9330 calibrating kit of tools).

e) Carrying out measurement of incident power P_I.
f) Careful placement of the cut-out sample inside the coaxial line and measurement of the reflection coefficient and transmitted power P_T.
g) The cut-out standard material (polytetrafluoroethylene - PTFE load of thickness 1 mm) was placed into the coaxial line and the reflection coefficient and transmitted power

Fig. 11 BF-TEM micrographs of hybrid filler Pr/Si 7 at different magnifications: **a** × 60,000; **b** ×400000
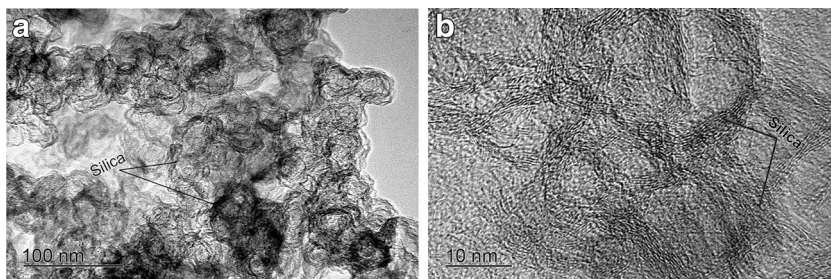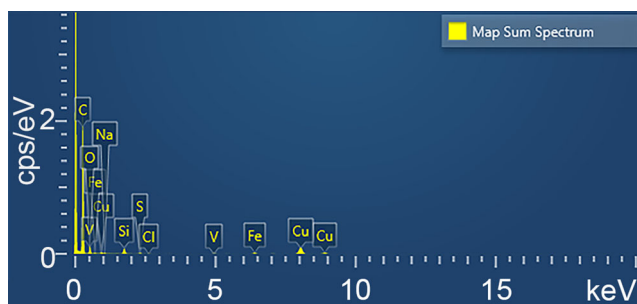
Fig. 12 Energy dispersive X-ray spectrum of hybrid filler Pr/Si 3

P_T measured for confirming the correctness of the measurements done.

The measurements were carried out at room temperature varying from 19 °C up to 24 °C and incident power P_I at the inlet of the coaxial measuring line varying from 800 μW up to 1300 μW within the frequency range of 1 GHz to 12 GHz.

Results and discussion

Characterization of the studied fillers

Printex XE-2B carbon black (from Orion Engineered Carbons GmbH) has been used as a substrate for the hybrid fillers studied due to its high conductivity, specific surface area, iodine adsorption (IA), oil absorption number, etc. Table 2 summarizes the main properties of the hybrid fillers obtained. The properties of the fillers we have modified are compared to those of Printex XE-2B carbon black as given in the data sheet of the product provided by the producers.

The oil absorption number (OAN) or dibutylphthalate absorption (DBPA) of the fillers reveals their ability to form secondary structures - aggregates and agglomerates. Therefore OAN is a key parameter for a great part of the fillers used in rubber industry [32, 33]. As seen from Table 2, the non-modified carbon black has OAN of 420 ml/100 g. The values of OAN for both carbon black/silica hybrid fillers (Pr/Si 3 and Pr/Si 7) obtained by impregnation of Printex XE-2B carbon black with different silicasol amounts are 460 and
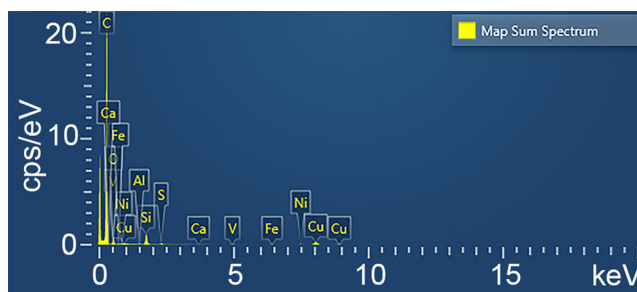

Fig. 13 Energy dispersive X-ray spectrum of hybrid filler Pr/Si 7

480 ml/100 g, respectively. That shows that, the hybrid fillers we have obtained are more prone to forming different secondary structures than non-modified Printex XE-2B carbon black. The fact is due to the silica available in the fillers. The effect is more pronounced at higher silica amounts in the total mass of the hybrid fillers. As known, silica is hydrophilic and has hydroxyl (silanol) groups over its surface. Silanol groups located over the silica particles interact with each other via hydrogen bonds what ensures them aptitude to agglomeration greater than that of carbon black.

The iodine adsorption (IA) of fillers reveals their adsorption activity. The method is applicable only to the characterization of carbon black [33]. For that reason IA values for the prepared hybrid fillers comprising certain amounts of silica presented in Table 2 are subjective.

As seen from Table 2, the specific surface area (BET) of non-modified Printex XE-2B carbon black is about 1000 m²/g. Its impregnation with different silicasol amounts (equivalent to 3 % and 7 % of silica, respectively) leads to gradual decrease of the specific surface area of the hybrid fillers. That decrease is caused by the lower specific surface area of silica phase.

Obviously the difference in silicasol amounts used for the modification is not great enough to cause drastic differences in the values for the adsorption-texture parameters of the hybrid fillers obtained. Nevertheless, Table 2 shows the synchronic (though insignificant) decrease of the total volume of Pr/Si 7 pores, if compared to that of Pr/Si 3. On the contrary, the average diameter of the pores is the same for both fillers what proves the identical process of forming the carbon/silica aggregates.

Figures 4, 5, 6 and 7 present the volume of adsorbed gas dependence (cm³/g) on relative pressure (p/p₀) and the derivative volume (dV) as a function of pore diameter (nm) of the studied fillers.

As seen from Figs. 4, 5, 6 and 7, the curves for the pores size distribution for both fillers are more or less of quite a similar pattern. Although, it could be assumed that, the major peaks at D_P: 25–65-70 nm for both fillers are due to inter-aggregate pores dominating in their structure. The availability of intra-aggregate pores is more pronounced in the case of Pr/Si 3, while in the case of Pr/Si 7 those are practically massively blocked by silicasol. That means, silica is located over the surface of carbon aggregates in Pr/Si 3, while in Pr/Si 7 the silica phase is distributed both over and inside the carbon black aggregates. Obviously, in the case of Pr/Si 7 aggregates clustering is more pronounced than in the case of Pr/Si 3. The occurrence of visible ill-resolved peaks for Pr/Si 7 (distribution curve) is related to the intra-cluster pores (in the clustered aggregates which are of large size than those of filler Pr/Si 3).

Doubtless, energy dispersive X-ray spectroscopy (XEDS), used at the scanning transmission electron microscopy (STEM), or STEM-XEDS, is the most appropriate modern method for answering questions about the distribution of carbon and silica phases within the hybrid filler obtained.

Fig. 14 **a** Bright field micrograph of FeS particle (in the middle) in hybrid filler Pr/Si 3; **b** Single crystal SAED pattern of FeS PDF 76–0961 in orientation [081]
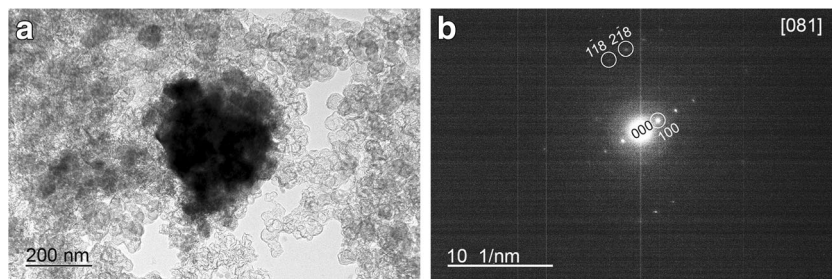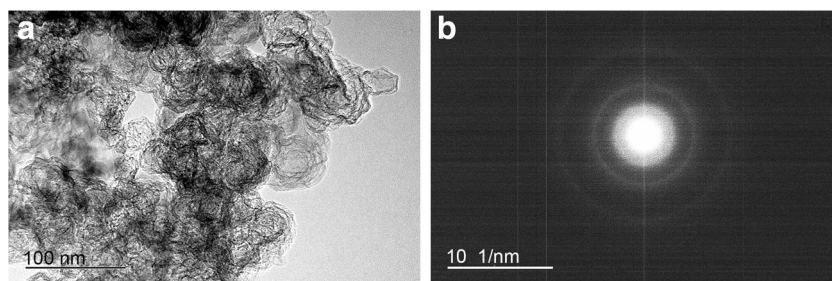

Figures 8 and 9 present the bright field STEM images and the compositional maps of the hybrid fillers studied.

Figures 8 and 9 confirm the successful modification of conductive Printex XE-2B carbon black with different silicasol amounts what has resulted into carbon black/silica hybrid fillers with a different quantitative ratio between the conductive (carbon) and dielectric (silica) phases. The compositional maps of the fillers obtained show that the silica phase is evenly distributed in that of Printex XE-2B carbon black in filler Pr/Si 3 (comprising 3 % of silica). In the case it is mainly distributed over the surface of carbon aggregates. There are larger lumps of the inorganic phase (clusters, agglomerates) and domains where silica is less in filler Pr/Si 7 (comprising 7 % of silica). That reveals the silica phase to be distributed over the surface of carbon black aggregates as well as inside them. STEM analysis is in agreement with the texture characteristics of the hybrid fillers investigated and evidences that, the distribution of silica phase in the carbon one in both fillers hinders at a certain extent the interaction between the conductive particles (i.e. the formation of conductive pathways). On the other hand, that could provide an easy control and tailoring of the microwave properties of the elastomer composites. That has been also confirmed by TEM micrographs of the hybrid fillers presented in Figs. 10 and 11.

As seen from TEM micrographs of higher magnifications (× 400,000), presented in Figs. 10b and 11b, in both hybrid fillers the darker and more ordered structures of silica are located over the surface of carbon black (the brighter structures). TEM micrographs of lower magnifications (Figs. 10a and 11a), prove the above statement about the distribution of the two phases in the hybrid fillers obtained which is based on their texture characteristics and STEM analysis.

Figures 12 and 13 present the Energy Dispersive X-ray spectra of the hybrid fillers studied. The figures show that, the fillers comprise traces of small amounts of vanadium, nickel, iron, etc. but carbon and silica. Those results are expected, as the metals are present in Printex XE-2B conductive carbon black used as a substrate for the fillers preparation.

Figures 14a and 15a present the bright field micrographs which show the morphologies of the particles, available in the hybrid fillers studied, involved in SAED (Selected Area Electron Diffraction) measurements (Figs. 14b and 15b).

SAED patterns shown in Figs. 14b and 15b confirm the availability of FeS and Fe_2O_3 (Powder Difraction File – PDF 76–0961, 84–0311) in the hybrid fillers studied. That evidences the existence of the above mentioned metals in the obtained products in the form of various sulfides and chiefly in the form of oxides. Regarding the aim of our investigations the result is positive since some of those oxides find application in manufacturing elastomer based EMI SM [14].

Microwave properties

Figures 16, 17 and 18 show measured total shielding effectiveness (SE_T), reflective shielding effectiveness (SE_R) and absorptive shielding effectiveness (SE_A) of the studied composites over the frequency range of 1 GHz to 12 GHz. The measurements were conducted on samples 2.71 mm (NR 1), 2.65 mm (NR 2) and 2.85 mm (NR 3) thickness.

As seen from Figs. 16, 17 and 18, sample NR 1 comprising non-modified Printex XE-2B has the lowest total shielding effectiveness (SE_T). The average SE_T value in the case is about 11.31 dB. In all cases the total shielding effectiveness of composites NR 2 and NR 3 comprising the studied hybrid
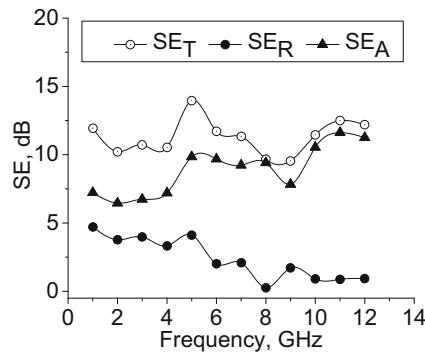
Fig. 15 Bright field micrograph of hybrid filler Pr/Si 7; **b** Polycrystalline SAED pattern of hybrid filler Pr/Si 7

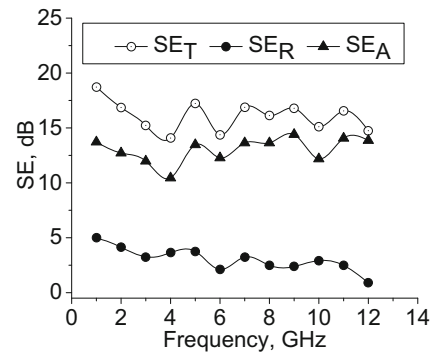**Fig. 16** Frequency dependence of SE_T, SE_R and SE_A of sample NR 1

Fig. 18 Frequency dependence of SE_T, SE_R and SE_A of sample NR 3

fillers is higher than that of composite NR 1 filled with their substrate carbon black. Moreover, with the increase in the silica amount in the total mass of the hybrid fillers the total shielding effectiveness of the composites studied improves. In the frequency range 1–12 GHz, the best SE_T was obtained for NR 3, with average value of 16.06 dB. Taking into account that, the reflective shielding effectiveness (SE_R) of the composites studied does not change significantly depending on the type of filler, the total shielding effectiveness has been determined by the changes in the absorptive shielding effectiveness (SE_A). As the figures show, SE_A of the composites studied increases with the increasing silica amount in the hybrid fillers. That is because of the inorganic (dielectric) phase of the fillers distributed both over the surface and inside the carbon black aggregates (conductive phase). Thus the interaction between the conductive particles (building of conductive pathways) is restricted what is in fact one of the prerequisites for obtaining microwave absorbers. The higher silica amount in the fillers the more pronounced the said effect is. Besides, with increasing silica amount in the total mass of the hybrid fillers probably the number of formed electric dipoles in the composites thus filled increases. That leads to a deeper penetration of the electromagnetic waves into the material and to an increase in latter's absorptive shielding effectiveness. The results obtained confirm fully our working hypothesis.

Figures 16, 17 and 18 reveal the resonance character of SE_T, SE_R and SE_A dependence on frequency. In all studied

cases absorption is a dominating mechanism. That could be explained examining in more details the values of the modulus of the reflection coefficient presented in Fig. 19. As seen, the modulus of the reflection coefficient for the composite filled with Pr/Si 3 (NR 2), for instance, at 1 GHz is 0.81. The amplitude of the reflected wave will be approximately 81 % of the incident wave. That means the power of the reflected wave ($P_R = |\varGamma|^2 \cdot P_I$, Fig. 1) will be 66 % of the power of the incident wave (P_I). According to Eq. (3), the reflective shielding effectiveness in that case is about 4.6 dB at 1 GHz. According to the law of conservation of energy the wave penetrating the sample will have power equal to 34 % of that of the incident wave. In accordance with Fig. 17 the total shielding effectiveness (SE_T) at 1 GHz is approximately 14 dB. As it is clear from Eq. (2), the transmitted power (P_T) is approximately 4 % of the incident power (P_I). According to Eq. (2) and (4), the low P_T value determines the high SE_A value and the dominating absorption character of the microwave shielding effectiveness.

The frequency dependence of the attenuation coefficient (α, dB/cm) of the studied composites is presented in Fig. 20. Obviously, the attenuation coefficient (which is a direct function of the absorptive shielding effectiveness) of the studied composites increases with the increasing silica amount in fillers they comprise. As the data in the figure shows, in the frequency interval from 1 GHz to 4 GHz the attenuation coefficient values for NR 3 decrease to 35 dB/cm approximately.
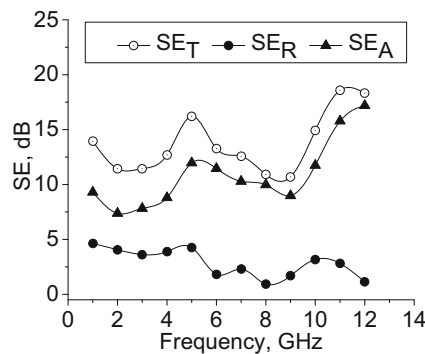

Fig. 17 Frequency dependence of SE_T, SE_R and SE_A of sample NR 2
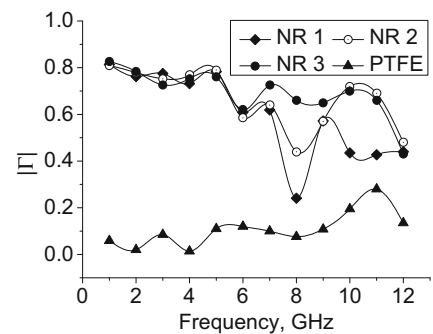

Fig. 19 Frequency dependence of the modulus of reflection coefficient $|\varGamma|$ of the studied composites
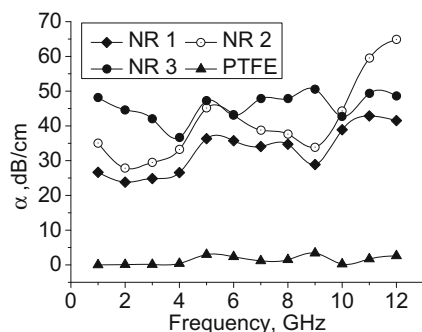
Fig. 20 Frequency dependence of the attenuation coefficient (α) of the studied composites

The increase in the attenuation coefficient values for NR 2 up to 65 dB/cm is observed with the increasing frequency from 9 GHz to 12 GHz exhibiting frequency selectivity in the X-band. The low almost zero values of the attenuation coefficient for the completely transparent for electromagnetic waves polytetrafluoroethylene confirm the correctness of the performed measurements.

The high conductivity of the studied composites determined by their high concentration (above the percolation threshold) of fillers wherein predominates the conductive phase, is the reason for their shielding effectiveness and for the impossibility to measure their dielectric properties. The conductive and dielectric properties of polymer materials depend on many factors and the filler/matrix ratio is amongst the most important ones. In the presence of small amounts of a conductive filler elastomer composites are good dielectric materials but above the critical filler concentration (percolation threshold) the conductivity may increase drastically [34]. Literature studies have established that, the EMI SE of a composite is a function of its electrical conductivity. Moreover, EMI SE of composites increases with the filler concentration [5, 35].

To verify the assumption that the composites studied possess high conductivity, they were placed successively at the
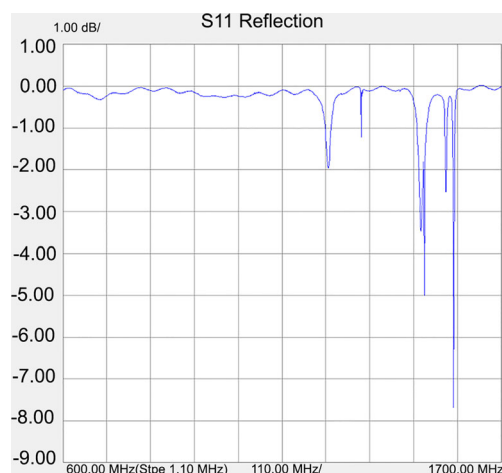

Fig. 22 S_{11} of the cavity containing sample NR 2

maximum of the electric field of a volume rectangular resonator. The cavity used for measurements was a rectangular waveguide with dimensions 207.5 mm (length), 248 mm (width) and 124 mm (height). A conducting plate with small aperture (38 mm) provided inductive coupling to the cavity with coaxial-waveguide transition. The sample under test was inserted into the center of the cavity (at peak electric field). Dimensions of the investigated samples (NR 2 and metal) were 1 mm (width), 0.5 mm (thickness) and 124 mm (height). The cavity operated in a TE_{101} mode with resonant frequency of 942.5 MHz. Measurements of S_{11} parameter were performed using an Agilent FieldFox N9212 network analyzer connected to the cavity. The S parameters of the empty cavity, the cavity with sample NR 2 and the metal sample are shown in Figs. 21, 22 and 23. Obviously, the insertion of the composite NR 2 causes collapse of TE_{101} mode (the electric field component). In the case of the cavity with a metal sample the results are almost the same (Fig. 23). That allows the conclusion that the composites studied comprising a high amount of conductive filler exhibit behaviour similar to that of the metals
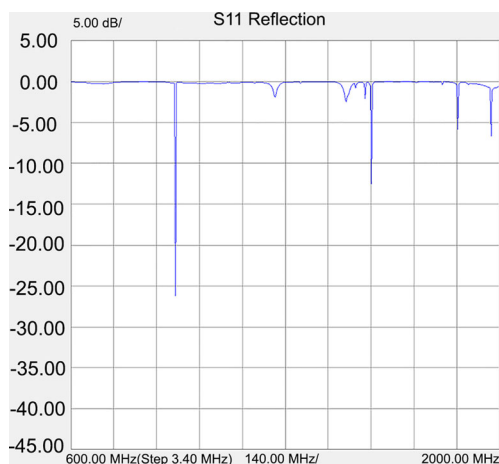

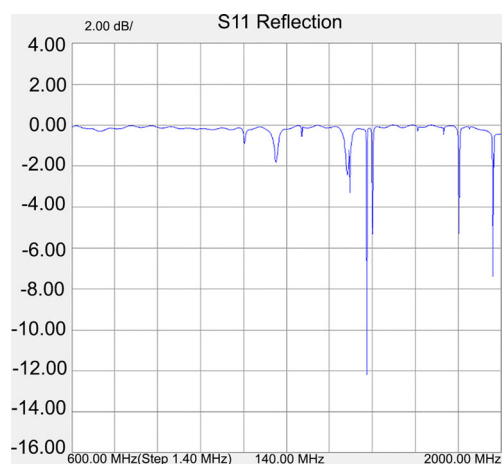**Fig. 21** S_{11} of the empty cavity

Fig. 23 S_{11} of the cavity containing the metal sample

when interacting with an electromagnetic wave in the frequency range form 0.9 GHz to 12 GHz. Kaynak and coworkers have observed the same results [5].

The investigations carried out reveal that the composites we have prepared have a good potential to be used for several applications such as antennas, automobiles, sensors and military-related applications.

Conclusions

The work reports on the synthesis of hybrid conductive carbon black/silica fillers and on their characterization by up-to-date methods. The results obtained show that, the silica (dielectric) phase is distributed both over the surface and inside the carbon black aggregates (conductive phase). Thus, the interaction between the particles of the conductive filler (building of conductive pathways) is restricted. The effect is more pronounced with the increasing silica amount in the hybrid fillers. The fillers obtained allow an easy control and tailoring of the elastomer based EMI SM. The composites filled with the hybrid filler comprising the highest amount of silica possess the best total shielding effectiveness and absorptive shielding effectiveness. In all cases absorption is the mechanism prevailing in effectiveness. Although the composites studied reflect the greater part of the power of the incident wave (about 66 %), the wave penetrating the samples has power about 34 % of the incident power. However, the transmitted power P_T is only 4 % of the incident wave (P_I) what in fact determines the absorption character of the achieved microwave shielding effectiveness. The high conductivity of the composites studies is the reason for the impossibility to measure their dielectric properties.

The investigations carried out reveal the good potential of the composites studied for finding applications as antennas, automobiles, sensors and military-related applications.

References

1. Ghasemi A, Liu X, Morisako A (2007) Magnetic and microwave absorption properties of BaFe12 − x (Mn0.5Cu0.5Zr)x/2O19 synthesized by sol–gel processing. J Magn Magn Mater 316(2):e105–e108. doi:10.1016/j.jmmm.2007.02.043
2. Yusoff AN, Abdullah MH, Ahmad SH, Jusoh SF, Mansor AA, Hamid SAA (2002) Electromagnetic and absorption properties of some microwave absorbers. J Appl Phys 92(2):876–882. doi:10.1063/1.1489092
3. Mottahed BD, Manoochehri S (1995) A review of research in materials, modeling and simulation, design factors, testing, and measurements related to electromagnetic interference shielding. Polymer-plastics technology and. Engineering 34(2):271–346. doi:10.1080/03602559508015827
4. Lakshmi K, John H, Mathew KT, Joseph R, George KE (2009) Microwave absorption, reflection and EMI shielding of PU–PANI composite. Acta Mater 57(2):371–375. doi:10.1016/j.actamat.2008.09.018
5. Kaynak A, Polat A, Yilmazer U (1996) Some microwave and mechanical properties of carbon fiber-polypropylene and carbon black-polypropylene composites. Mater Res Bull 31(10):1195–1206. doi:10.1016/0025-5408(96)00124-9
6. Lu G, Li X, Jiang H (1996) Electrical and shielding properties of ABS resin filled with nickel-coated carbon fibers. Compos Sci Technol 56(2):193–200. doi:10.1016/0266-3538(95)00143-3
7. Chung DDL (2001) Electromagnetic interference shielding effectiveness of carbon materials. Carbon 39(2):279–285. doi:10.1016/S0008-6223(00)00184-6
8. Rahaman M, Chaki TK, Khastgir D (2011) Development of high performance EMI shielding material from EVA, NBR, and their blends: effect of carbon black structure. J Mater Sci 46(11):3989–3999. doi:10.1007/s10853-011-5326-x
9. Chiang W-Y, Cheng K-Y (1997) Processing conditions for electromagnetic interference shielding effectiveness and mechanical properties of acrylonitrile-butadiene-styrene based composites. Polym Compos 18(6):748–756. doi:10.1002/pc.10327
10. Sahoo B, Naskar K, Tripathy D (2012) Conductive carbon black-filled ethylene acrylic elastomer vulcanizates: physico-mechanical, thermal, and electrical properties. J Mater Sci 47(5):2421–2433. doi:10.1007/s10853-011-6065-8
11. Miyata Y, Matsumoto M (1997) Two-layer wave absorber composed of soft-magnetic and ferroelectric substances. IEEE Trans Magn 33(5):3427–3429. doi:10.1109/20.617966
12. Feng Y, Qiu T, Li X, Shen C (2007) Microwave absorption properties of the carbonyl iron/EPDM radar absorbing materials. J Wuhan Univ Technol 22(2):266–270. doi:10.1007/s11595-005-2266-9
13. Barba AA, Lamberti G, d'Amore M, Acierno D (2006) Carbon black/silicone rubber blends as absorbing materials to reduce electro magnetic interferences (EMI. Polym Bull 57(4):587–593. doi:10.1007/s00289-006-0598-z
14. Krishnan Y, Chandran S, Usman N, Smitha TR, Parameswaran PS, Prema KH (2015) Processability, mechanical and magnetic studies on natural rubber- ferrite composites. International journal of chemical. Studies 3(1):15–22
15. Ismail H, Sam ST, Mohd Noor AF, Bakar AA (2007) Properties of ferrite-filled natural rubber composites. Polymer-plastics technology and. Engineering 46(6):641–650. doi:10.1080/03602550701305054
16. Kong I, Hj Ahmad S, Hj Abdullah M, Hui D, Nazlim Yusoff A, Puryanti D (2010) Magnetic and microwave absorbing properties of magnetite–thermoplastic natural rubber nanocomposites. J Magn Magn Mater 322(21):3401–3409. doi:10.1016/j.jmmm.2010.06.036
17. Urogiova E, Hudec I, Bellusova D (2006) Magnetic and mechanical properties of strontium ferrite – rubber composites. Kautschuk gummi. Kunststoffe:224–228
18. Dishovsky N (2009) Rubber based composites with active behaviour to microwaves (review). Journal of the University of Chemical Technology and Metallurgy 44(2):115–122
19. Cao M-S, Song W-L, Hou Z-L, Wen B, Yuan J (2010) The effects of temperature and frequency on the dielectric properties, electromagnetic interference shielding and microwave-absorption of short carbon fiber/silica composites. Carbon 48(3):788–796. doi:10.1016/j.carbon.2009.10.028
20. Wen B, Cao M-S, Hou Z-L, Song W-L, Zhang L, M-M L, Jin H-B, Fang X-Y, Wang W-Z, Yuan J (2013) Temperature dependent microwave attenuation behavior for carbon-nanotube/silica composites. Carbon 65(0):124–139. doi:10.1016/j.carbon.2013.07.110
21. Yuan X, Cheng L, Zhang L (2014) Influence of temperature on dielectric properties and microwave absorbing performances of

TiC nanowires/SiO2 composites. Ceram Int 40 (10, Part A):15391–15397. doi:10.1016/j.ceramint.2014.05.080

22. Wang MJ, Kutsovsky Y, Zhang P, Mehos G, Murphy LJ, Mahmud K (2002) Using carbon-silica dual phase filler improve global compromise between rolling resistance, wear resistance and wet skid resistance for tires. Kautschuk gummi. Kunststoffe 55:33–40

23. Jana PB, Mallick K, De SK (1992) Effects of sample thickness and fiber aspect ratio on EMI shielding effectiveness of carbon fiber filled polychloroprene composites in the X-band frequency range. IEEE Trans Electromagn Compat 34(4):478–481. doi:10.1109/15.179281

24. Paul CR (2006) Introduction to electromagnetic compatibility, Second edn. John Wiley & Sons, Inc., Hoboken

25. Ott HW (2009) Electromagnetic compatibility engineering, First edn. John Wiley & Sons, Inc., Hoboken

26. Hernandez B (2013) Effect of graphitic carbon nanomodifiers on the electromagnetic shielding effectiveness of linear low density polyethylene nanocomposites. The Graduate School of Clemson University. South Carolina, USA

27. Srikanth VVSS, Raju KCJ (2015) Graphene/polymer nanocomposites as microwave absorbers. In: Sadasivuni KK, Ponnamma D, Kim J, Thomas S (eds) Graphene-Based Polymer Nanocomposites in Electronics Springer Series on Polymer and Composite Materials, First edn Springer International Publishing, Switzerland, pp 307–343. doi:10.1007/978-3-319-13875-6_12

28. Sung-Hoon P, Theilmann PT, Asbeck PM, Bandaru PR (2010) Enhanced electromagnetic interference shielding through the use of functionalized carbon-nanotube-reactive polymer composites. IEEE Trans Nanotechnol 9(4):464–469. doi:10.1109/TNANO.2009.2032656

29. Hong YK, Lee CY, Jeong CK, Lee DE, Kim K, Joo J (2003) Method and apparatus to measure electromagnetic interference shielding efficiency and its shielding characteristics in broadband frequency ranges. Rev Sci Instrum 74(2):1098–1102. doi:10.1063/1.1532540

30. Więckowski TW, Janukiewicz JM (2006) Methods for evaluating the shielding effectiveness of textiles. Fibres & Textiles in Eastern Europe 14(5 (59)):18–22

31. Chen LF, Ong CK, Neo CP, Varadan VV, Varadan VK (2004) Microwave electronics: Measurement and materials characterization, First edn. John Wiley & Sons, Ltd., Chichester

32. Donnet J-B, Custodero E (2013) Reinforcement of elastomers by particulate fillers. In: Mark JE, Erman B, Roland CM (eds) The Science and Technology of Rubber Fourth Edition edn Academic Press, Boston, pp 383–416. doi:10.1016/B978-0-12-394584-6.00008-X

33. Rodgers B, Waddell W (2013) The science of rubber compounding. In: Mark JE, Erman B, Roland CM (eds) The Science and Technology of Rubber. Fourth Edition edn. Academic Press, Boston, pp 417–471. doi:10.1016/B978-0-12-394584-6.00009-1

34. Joy J, Tresa Sunny A, Mathew LP, Pothen LA, Thomas S (2014) Micro and nano metal particle filled natural rubber composites. In: Thomas S, Chan CH, Pothen LA, Joy J, Maria H (eds) Natural Rubber Materials, Composites and Nanocomposites, vol 2, vol 2. First edn. The Royal Society of Chemistry, Cambridge, United Kingdom, pp. 307–325. doi:10.1039/9781849737654–00307

35. Kang G-H, Kim S-H (2014) Electromagnetic wave shielding effectiveness based on carbon microcoil-polyurethane composites. Journal of Nanomaterials 2014:6. doi:10.1155/2014/727024